



OPEN

Discovery of uncompetitive inhibitors of SapM that compromise intracellular survival of *Mycobacterium tuberculosis*

Paulina Fernández-Soto¹, Joshua Casulli^{1,2,3}, Danilo Solano-Castro¹, Pablo Rodríguez-Fernández¹, Thomas A. Jowitt^{1,3}, Mark A. Travis^{1,2,3}, Jennifer S. Cavet¹ & Lydia Taberero^{1,2}✉

SapM is a secreted virulence factor from *Mycobacterium tuberculosis* critical for pathogen survival and persistence inside the host. Its full potential as a target for tuberculosis treatment has not yet been exploited because of the lack of potent inhibitors available. By screening over 1500 small molecules, we have identified new potent and selective inhibitors of SapM with an uncompetitive mechanism of inhibition. The best inhibitors share a trihydroxy-benzene moiety essential for activity. Importantly, the inhibitors significantly reduce mycobacterial burden in infected human macrophages at 1 μ M, and they are selective with respect to other mycobacterial and human phosphatases. The best inhibitor also reduces intracellular burden of *Francisella tularensis*, which secretes the virulence factor AcpA, a homologue of SapM, with the same mechanism of catalysis and inhibition. Our findings demonstrate that inhibition of SapM with small molecule inhibitors is efficient in reducing intracellular mycobacterial survival in host macrophages and confirm SapM as a potential therapeutic target. These initial compounds have favourable physico-chemical properties and provide a basis for exploration towards the development of new tuberculosis treatments. The efficacy of a SapM inhibitor in reducing *Francisella tularensis* intracellular burden suggests the potential for developing broad-spectrum antivirulence agents to treat microbial infections.

Tuberculosis (TB) is still a major global health threat with 10 million people developing active TB and over 1.5 million deaths every year¹. Current TB treatments are long (6–9 months) with multiple drugs that cause severe hepatotoxicity and other serious side effects. In addition, the emergence of drug resistance is now a major challenge as effective treatments are lacking. Two recent new drugs, bedaquiline² and delamanid³ were approved for the treatment of multidrug-resistant TB (MDR-TB). However, resistance to both drugs was reported in less than a year after clinical use^{4,5}, and the number of cases continue to rise^{6,7}. The increase of MDR-TB and extremely drug resistant TB (XDR-TB) cases underlines the need to develop new drugs with novel mechanisms of action.

Antivirulence agents differ from conventional antibiotics in that they do not target bacterial growth directly, instead they block virulence factors that cause host damage and disease⁸. Targeting bacterial virulence is a non-traditional strategy that is gaining momentum for the treatment of microbial infections^{8–11}. Recent reports have confirmed the efficacy of antivirulence agents on reducing burden of *Mycobacterium tuberculosis* (Mtb), the causative agent of TB, in vitro^{12–16} and in vivo^{17,18}. However, antivirulence agents have yet to be incorporated in the TB drug development pipeline^{19–21}.

SapM, is a secreted alkaline phosphatase from Mtb²², and an attractive target to exploit antivirulence strategies. Previous studies have demonstrated that SapM is essential for arresting phagosomal maturation^{23,24}, a critical event to prevent the antimicrobial function of the macrophage thus enabling mycobacterial survival and

¹School of Biological Sciences, Faculty of Biology Medicine and Health, Manchester Academic Health Science Centre, University of Manchester, Manchester M13 9PT, UK. ²Lydia Becker Institute for Immunology and Inflammation, University of Manchester, Manchester, UK. ³Wellcome Centre for Cell-Matrix Research, University of Manchester, Manchester, UK. ✉email: Lydia.Taberero@manchester.ac.uk

Library	Number screened	Primary screening ($\geq 50\%$ inhibition)	Hits confirmed ($\geq 50\%$ inhibition)	IC ₅₀ ($< 10 \mu\text{M}$)
In-house	96	0	–	–
LOPAC-Pfizer	90	1	0	–
Enzo-BML 2834	32	3	1	0
LOPAC-1280	1273	14	5	2
SAR	12	–	4	1
Total	1503	18	10	3

Table 1. Summary of compounds screened from commercial and in-house libraries and structure–activity relationship (SAR) analyses.

persistence. Furthermore, guinea pigs infected with the ΔsapM Mtb strain showed total absence of mycobacteria in lungs and spleen at 16 weeks post infection, demonstrating the critical role of SapM in Mtb pathogenesis²⁴. Importantly, the lungs, liver and spleens of these animals showed only few tubercles, negligible histopathological tissue damage, and all the infected animals survived the infection²⁴. Clearly, the role of SapM is important for Mtb persistence, but it also impacts on the host ability to fight the infection. Our hypothesis is that if we could block the action of SapM with a small molecule, we may be able to enhance infection clearance and help to improve TB treatments.

The *sapM* gene is unique in the mycobacterial genome and there is no human orthologue to SapM^{22,25}, suggesting the potential to develop specific and selective inhibitors. Recently, we have reported that SapM can be inhibited using L-ascorbic acid (L-AC) and 2-phospho-L-ascorbic acid (2P-AC), and that inhibition reduced mycobacterial survival in human THP1 macrophages²². However, these are low potency inhibitors with IC₅₀ values $> 200 \mu\text{M}$.

Here we have screened 1503 compounds from commercial and in-house libraries and identified three new potent (IC₅₀ $< 10 \mu\text{M}$) and selective inhibitors of SapM that behave as uncompetitive inhibitors. These compounds significantly reduce up to 70% of Mtb burden in human THP-1 macrophages at a low concentration of $1 \mu\text{M}$. Two of these inhibitors are characterised by a benzylidenemalononitrile scaffold and share a tryhydroxy-benzene moiety with the third inhibitor, a Gallic acid derivative. The most potent inhibitor, compound **1**, also reduces the burden of *Francisella tularensis* in MH-S macrophages. *F. tularensis* is the causative agent of the lethal disease tularaemia²⁶ and secretes the virulence factor AcpA^{27–29}, a homologue of SapM that shares the same mechanism of catalysis and inhibition²². Our results demonstrate the potential of exploiting antivirulence agents to impair bacterial intracellular survival for the treatment of TB, with possible applications to other microbial infections.

Results and discussion

To identify new inhibitors of SapM, we screened four different compound libraries covering a wide range of pharmacological active drugs (LOPAC-1280 and LOPAC-Pfizer), phosphatase inhibitors (Enzo-BML-2834), and in-house compounds from other drug discovery programmes. A total of 1491 compounds were initially screened for activity against SapM. The primary screening resulted in a total of 18 compounds that reduced SapM specific activity (SA) by $\geq 50\%$ at $100 \mu\text{M}$ (Table 1, Fig. 1A). These compounds were re-purchased and re-tested to confirm their activity. Six of the re-tested compounds showed $\geq 50\%$ inhibition of SapM (Table 2, Fig. 1B). False positives or negatives are expected as compounds tend to degrade or precipitate after long-term storage in DMSO³⁰, but the number of hits identified in our screening is similar with previous reports using the same libraries^{31,32}.

The distribution of compound activity on SapM is homogeneous across the libraries (Fig. 1A), indicating an unbiased screening. Of note, some compounds increased the SA of SapM, an effect reported for allosteric activators³³. In total, six compounds (**1–6**), five from the LOPAC-1280 library and one from the Enzo-BML-2834, were considered for further analyses (Table 2). These compounds are reported to target different proteins: Tyrphostin 51 and HI-TOPK-32 are kinase inhibitors^{34,35}, RWJ-60475 is a tyrosine phosphatase inhibitor³⁶, Galloflavin is a lactate dehydrogenase inhibitor³⁷, YM-26734 is a phospholipase A2 inhibitor³⁸ and (6R)-BH4, Sapropterin dihydrochloride, is a cofactor for nitric oxide synthesis³⁹ used in the clinic to treat pulmonary hypertension⁴⁰.

Structure–activity relationship for SapM inhibitors. Among the six inhibitors, three compounds: Tyrphostin 51 (**1**), Galloflavin (**2**) and YM-26734 (**3**) completely abolished the enzymatic activity of SapM, and share the presence of a trihydroxy-benzene group (Table 2), also present in polyphenols reported as phosphatase inhibitors⁴¹. In order to gain structure–activity relationship (SAR) insight we searched for related compounds to **1** and **2** in the libraries tested and for commercially available derivatives. Compound **3** was not included in this search because of its complexity and poor drug-like properties according to the Lipinski's rule of five (Ro5)⁴².

We found six additional tyrphostins related to compound **1** (**7–12** in Table S1): five from the LOPAC-1280 library (**7–11**), and one from the Enzo-BML-2834 library (**12**). All six tyrphostins showed poor activity towards SapM at $100 \mu\text{M}$ (SA $> 73\%$). Another seven tyrphostins (**13–19**) were identified through searches in SciFinder (<https://scifinder.cas.org>) and tested for inhibition of SapM. Of these, **13** and **14** completely abolished enzyme activity at $100 \mu\text{M}$ (Table S1).

Additionally, nine compounds containing hydroxyl-substituted benzene rings were identified from the primary screening (**20–28** in Table S1), where **20** and **25** exhibited $\sim 30\%$ reduction in SA and the rest had poor or no activity (Table S1). A group of polyphenols found in the literature⁴¹ (**29–33**), including catechins and

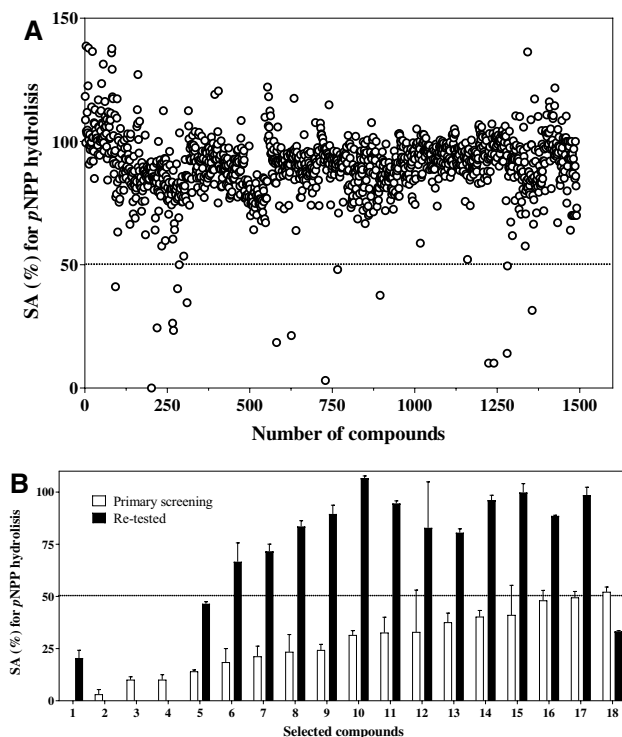


Figure 1. Primary screening of compounds. Enzymatic activity of SapM was assessed using the *p*NPP assay and expressed as percentage of specific activity (% SA). (A) Plot showing the effect of 1491 compounds at 100 μ M on SapM activity (compounds ordered from left to right as LOPAC-1280, Enzo-BML-2834, LOPAC-Pfizer and in-house). Compounds that reduced SA by $\geq 50\%$ (black dotted line) were selected. (B) Bar graph showing effect on SA of selected compounds from the primary screening (A) (bars in white) and re-tested compounds (bars in black). SA values of 0% overlap the x-axis. Percentage of SA is calculated relative to the *p*NPP DMSO control. Error bars indicate \pm standard deviation of the mean (SD) of duplicates.

procyanidins, were tested for inhibition of SapM. Of these, **29** and **30** showed inhibition of SapM activity of about 70 and 40%, respectively (Table S1).

All tyrphostins tested (**1**, **7–19**), except **11**, contain a *cis*-benzylidenemalononitrile core³⁴ (Fig. 2A) that mimics the moieties of tyrosine and erbstatin⁴³, and one or more hydroxyl substitutions on the benzene ring, and variations in the side chain. The position of the nitrile groups or the length of the side chain, do not appear to impact on SapM inhibition. For instance, the same potency is observed for **1** and **13**, where the position of the nitrile group changes from C4 to C3, and with similar potency to **14**, with only two carbons in the side chain instead of four (Fig. 2A, Suppl. Table S1).

However, the number of hydroxyl groups (–OH) in the benzyl ring of tyrphostins, has a substantial contribution to potency because removal of one or more –OH results in loss of inhibition (Table S1). Compounds **1**, **13** and **14**, with three –OH abolished enzyme activity completely, whereas **7**, **15** and **16** with two –OH only inhibit by ~ 30 –50% and **8**, **9** and **12** with one –OH inhibit by less than 21%.

For other hydroxyl-substituted benzene compounds it is clear that the presence of –OH alone is not sufficient for full potency. Compound **2** with three –OH inhibits SapM activity completely at 100 μ M, but **26**, **28**, **31–33** with more than three –OH show none or poor activity (Suppl. Table S1). Thus, the presence of at least two –OH, appears to be necessary for inhibition particularly for the benzylidenemalononitrile scaffold, but not sufficient for full potency.

Potency and selectivity of SapM inhibitors. IC_{50} values of key compounds showing substantial inhibition on SapM in the primary and SAR screens were determined using dose–response curves (Fig. 2B). Compound **4** was not used as it precipitates at > 100 μ M, preventing the ability to reach saturation. The more potent compounds are **1**, **2**, **13** and **14**, with IC_{50} values ranging from 6 to 14 μ M (Fig. 2B, Table 3). These compounds are up to 40 times more potent than the 2P-AC and L-AC inhibitors that we have previously reported ($IC_{50} > 200$ μ M)²². Furthermore, all inhibitors show selectivity towards SapM over other secreted phosphatases in Mtb (Table 3): MptpB, a lipid phosphatase with a similar mode of action to SapM^{18,44} and MptpA, a tyrosine phosphatase that regulates phagosome acidification^{45–47}. Importantly, compounds **1**, **2**, and **13** are also selective over the human phosphatases PTP1B (phosphotyrosine specific) and VHR (dual specificity phosphatase) (Table 3).

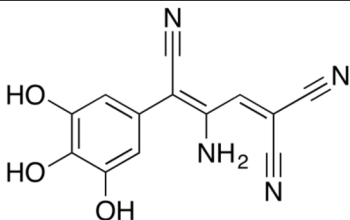
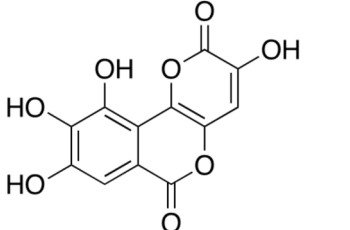
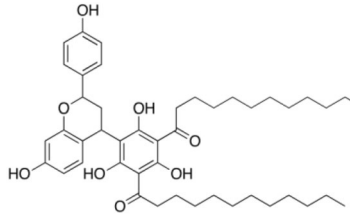
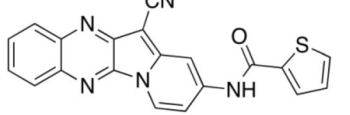
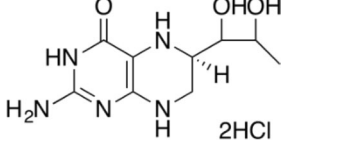
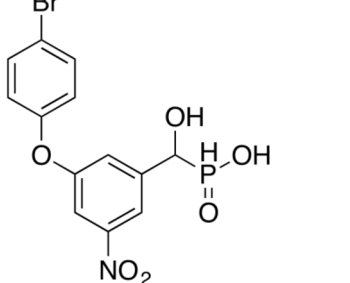
N	Compound name	Structure	%SA
1	Tyrphostin 51		0
2	Galloflavin		0
3	YM-26734		0
4	HI-TOPK-32		20.5 ± 3.7
5	(6R)-BH4		33.3 ± 0.3
6	RWJ-60475		46.6 ± 0.9

Table 2. Hits identified in primary screen. Percentage specific activity (SA) of compounds tested against SapM at 100 μM . Values are average \pm SD of duplicates.

SapM inhibitors show an uncompetitive mechanism of inhibition. Kinetics studies showed that the best four inhibitors, **1**, **2**, **13** and **14**, behave as uncompetitive inhibitors, as indicated by the characteristic pattern of parallel lines in the Lineweaver–Burk plots (Fig. 2C), where increasing amounts of inhibitor causes a reduction of both the K_m and V_{max} values⁴⁸. Uncompetitive compounds bind to the enzyme–substrate complex instead of the free enzyme⁴⁸. The potency of uncompetitive compounds is then enhanced as the substrate concentration in the reaction increases^{49,50}. This mechanism is similar to the one we observed for L-AC²², indicating a general mechanism of inhibition for this target.

SapM inhibitors reduce mycobacterial burden in vitro. Compounds with $\text{IC}_{50} < 10 \mu\text{M}$ (Table 3) were chosen to evaluate their efficacy in THP-1 macrophages infected with the Mtb H37Rv strain. Treatment with **1**, **2** and **13** at 1 μM and 40 μM resulted in a significant ($***p < 0.0001$) reduction of Mtb intracellular burden in

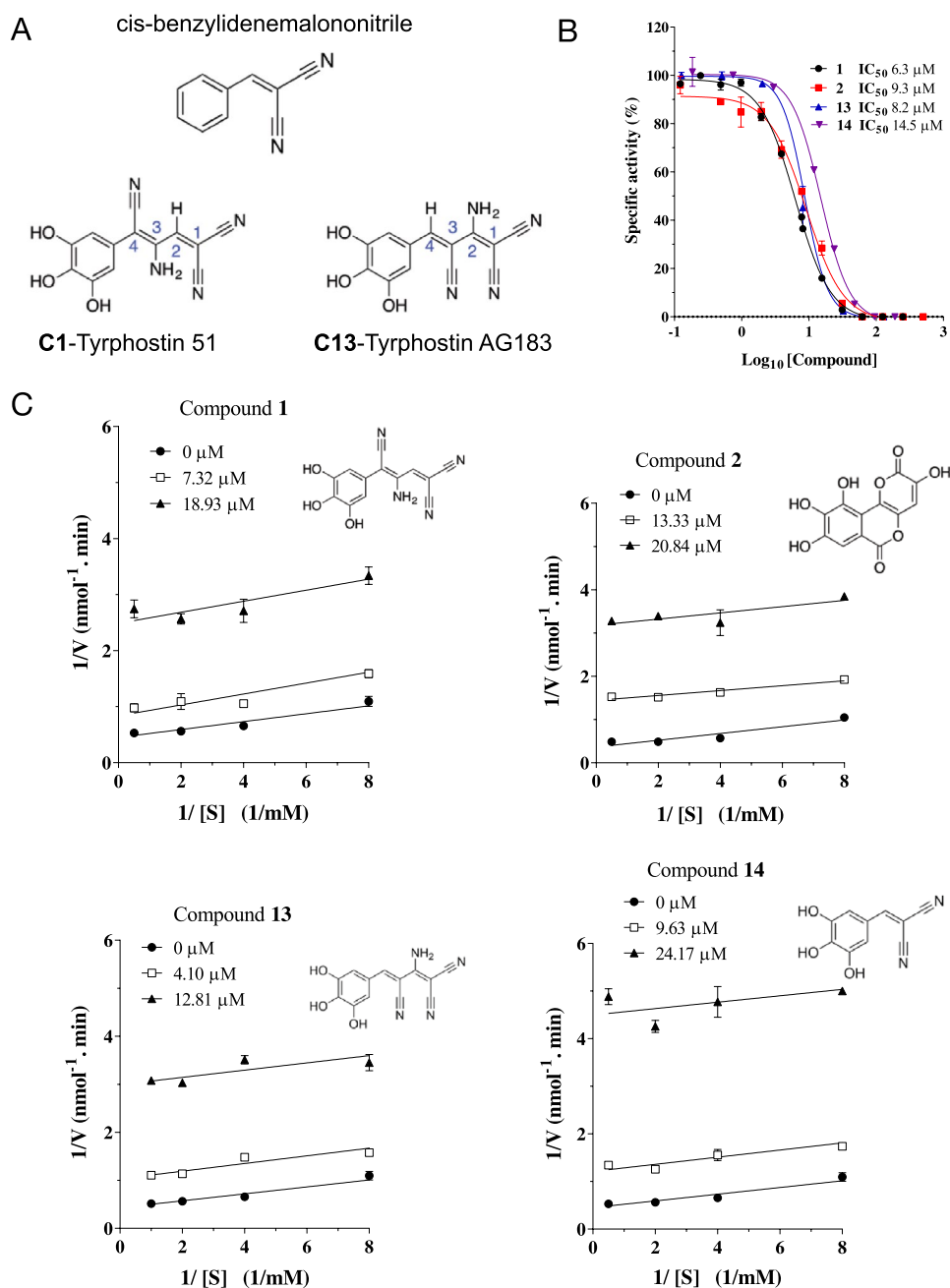


Figure 2. Dose–response curves and mode of inhibition for selected compounds. Compounds **1**, **2**, **13** and **14** were tested using the *p*NPP assay. **(A)** Common cis-benzylidenemalononitrile scaffold structure of the tyrphostin inhibitors and two examples compound **1** (C1) and **13** (C13). **(B)** Percentage of specific activity is calculated relative to the amount of *p*-nitrophenol released in the absence of inhibitor. Error bars represent \pm SD of two independent experiments. **(C)** Mechanism of inhibition of SapM. Lineweaver–Burk plots for **1**, **2**, **13** and **14**. Error bars represent \pm SD of triplicates.

resting THP-1 macrophages at 24 h and 72 h post infection when compared to DMSO controls (Fig. 3A,B). This reduction is comparable to that observed when deleting the *sapM* gene²⁴, and consistent with the critical role of SapM in intracellular mycobacterial survival^{23,24}. A similar effect is observed both in vitro^{12,13} and in vivo^{17,18}, when inhibiting MptpB, another secreted virulence factor involved in phagosomal maturation.

There is no substantial difference between treatment with **1** or **13**, with similar IC_{50} , suggesting that the change in the nitrile position in the benzylidenemalononitrile core does not influence efficacy in cells. Compound **2** is marginally better than **1** and **13** at 24 h but the differences are not statistically significant. The efficacy of these compounds is more pronounced at 24 h, with reductions of 50–70% on Mtb burden, compared to 30–50% at 72 h. This would agree with the proposed role of SapM in the dephosphorylation of PI(4,5) P_2 and PI3P during phagocytosis²², at the initial stages of the infection. Efficacy is also superior to the one we observed for MptpB

Compound number	IC ₅₀ (μM)				
	SapM	MptpA	MptpB	PTP1B	VHR
1	6.3 ± 1.0	19.8 ± 1.0	>100	>100	>100
2	9.3 ± 1.1	55.2 ± 1.1	>100	>100	>100
3	19.8 ± 1.1	>100	>100	–	–
4	ND	–	–	–	–
5	73.9 ± 1.2	–	–	–	–
6	41.9 ± 1.1	>100	>100	–	–
13	8.2 ± 1.0	16.7 ± 1.0	>100	>100	>100
14	14.5 ± 1.0	23.7 ± 1.1	>100	–	–
15	78.42 ± 2.7	–	–	–	–
29	63.0 ± 1.5	>100	>100	–	–

Table 3. Selectivity of SapM inhibitors towards phosphatases. Inhibition of selected compounds towards mycobacterial secreted phosphatases SapM, MptpA and MptpB, and human phosphatases PTP1B and VHR. IC₅₀ values are mean ± SD of two independent experiments. ND not determined as compound precipitates at concentrations > 100 μM.

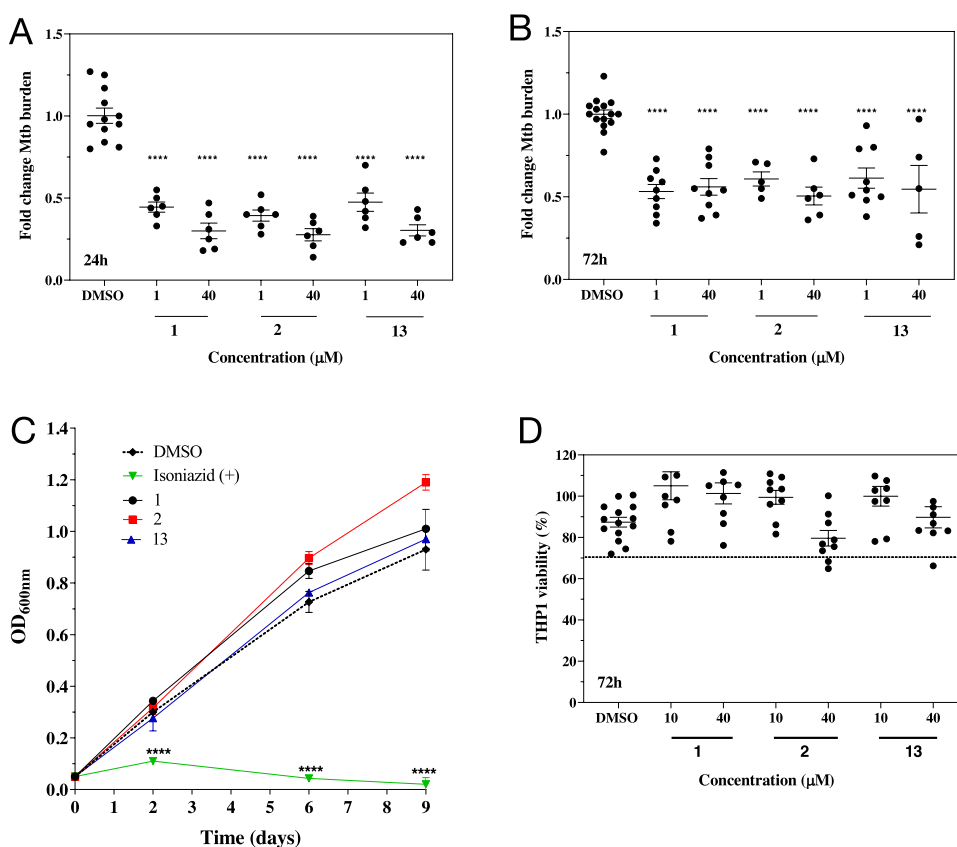


Figure 3. Effect of SapM inhibitors 1, 2 and 13 on Mtb H37Rv growth and intracellular burden. Efficacy of compounds at 1 and 40 μM on Mtb intracellular burden in THP-1 macrophages at 24 h (A) and 72 h (B) post infection. Fold change of Mtb burden was calculated from the average CFU/ml relative to the DMSO control (**** $p < 0.0001$). Error bars in (A,B) indicate ± SD of two and three independent experiments, respectively. (C) Effect of compounds at 40 μM on the acellular growth of Mtb in Middlebrook 7H9 broth monitored over 9 days using optical density (OD₆₀₀). DMSO and the first-line antibiotic isoniazid (at 0.14 μg/ml) were used as negative and positive controls, respectively. Error bars indicate ± SD of triplicates. Statistical significance was evaluated by two-way ANOVA (Dunnnett's test) compared to DMSO control (**** $p < 0.0001$). (D) THP-1 macrophage viability at 72 h upon treatment with compounds at 10 and 40 μM. Percentage of viability was calculated relative to the control (RPMI media only). Dashed black line indicates 70% viability. Error bars indicate ± SD of three independent experiments.

N	MW (Da)	HBA	HBD	LogP	HAC	TPSA (Å ²)	Solubility (mg/ml)
1	268.2	6	4	-1.38	20	158.08	5.2
2	278.2	8	4	-0.28	20	141.34	1.3
13	268.2	6	4	-1.38	20	158.08	5.2

Table 4. Predicted physico-chemical properties of the best SapM inhibitors obtained from SwissADME⁵¹. MW molecular weight, HBA number of hydrogen bond acceptors, HBD number of hydrogen-bond donors, LogP partition coefficient, HAC heavy atoms count, TPSA total polar surface.

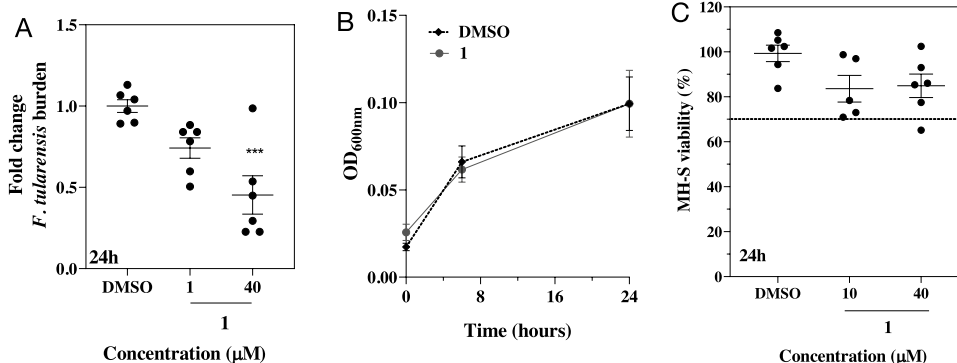


Figure 4. Effect of compound 1 on *F. tularensis* growth and intracellular burden. (A) Dose dependent efficacy of compound 1 on *F. tularensis* intracellular burden in MH-S macrophages at 24 h post infection. Bacterial burden was calculated from the average CFU/ml relative to DMSO control. Statistical significance was evaluated by one-way ANOVA (Dunnett's test) compared to DMSO control (***) $p < 0.001$. Error bars indicate \pm SD of two independent experiments. (B) MH-S cells viability in percentage at 24 h post treatment with compound 1. Percentage of viability was calculated relative to the control (RPMI media only). Dashed black line indicates 70% viability. Error bars indicate \pm SD of three independent experiments. (C) Effect of compound 1 on the acellular growth of *F. tularensis* monitored over 24 h using optical density (OD₆₀₀). Cultures were treated with 40 μM of the inhibitor. Negative control is DMSO. Error bars indicate \pm SD of triplicates.

inhibitors, which showed similar reduction of Mtb burden at concentrations of 80 μM or higher, instead of 1 μM^{12,18}.

None of the inhibitors tested affected acellular growth over the course of 9 days compared to the DMSO control (Fig. 3C). This is in agreement with previous reports (and our own data in Suppl. Fig. S1) that deletion of *sapM* impairs mycobacterial survival in macrophages and animal models of infection, but does not reduce growth in culture medium²⁴. Furthermore, the compounds had no significant effect on the intracellular burden of Δ *sapM* (Suppl. Fig. S1), supporting specificity.

The compounds showed no cytotoxicity (>70% viability) up to 40 μM in THP-1 macrophages for 72 h (Fig. 3D).

Compounds 1, 2 and 13 exhibit favourable drug-like properties (Table 4). The physico-chemical properties calculated with the SwissADME tool⁵¹ indicate that 1, 2 and 13 are relatively small molecules (Mw < 300 Da), highly hydrophilic, with predicted good solubility and with lead-like properties according to the Ro5 criteria⁴². Thus this makes them suitable candidates for further development and future validation in vivo. Binding of 1, 2 and 13 to SapM was confirmed by microscale thermophoresis (MST) (Suppl. Figs. S2, S3).

Compound 1 reduces *Francisella tularensis* intracellular burden. One of the closest homologues of SapM is the secreted phosphatase AcpA from *Francisella tularensis*, which acts as a virulence factor for that bacterium^{27,29}. We have demonstrated that SapM and AcpA share the same mechanism of catalysis²². We have also shown that AcpA inhibitors 2-PAC and L-AC, which reduce *F. tularensis* burden in vitro⁵², also inhibit SapM activity, and that 2-PAC significantly reduces intracellular survival of Mtb²². We hypothesized that SapM inhibitors may therefore have efficacy in reducing intracellular burden of *F. tularensis*. For this, the most potent compound 1 was confirmed to inhibit AcpA (Suppl. Methods and Suppl. Fig. S4) and selected to evaluate its efficacy in MH-S cells infected with *F. tularensis*.

As for Mtb, compound 1 reduces *F. tularensis* intracellular burden in a dose dependent manner, with a significant reduction (55%, *** $p < 0.001$) at 40 μM at 24 h post infection (Fig. 4A). Compound 1 is not cytotoxic to MH-S cells (>70% viability) (Fig. 4B), and does not affect acellular growth of *F. tularensis* (Fig. 4C). The efficacy of compound 1 in reducing Mtb and *F. tularensis* burden in infected macrophages suggests the potential of developing antivirulence agents with a broad-spectrum activity to treat microbial infections.

Conclusions

In this study we have identified new potent inhibitors of SapM ($IC_{50} < 10 \mu\text{M}$) that have an uncompetitive mechanism of inhibition. The inhibitors are specific to SapM and selective over other Mtb secreted phosphatases and human phosphatases. The best inhibitors **1** and **13**, contain a benzylidenemalononitrile core and share a trihydroxy-benzene group with compound **2**, also found in other polyphenol phosphatase inhibitors. Importantly, the best inhibitors, show significant efficacy in reducing intracellular Mtb burden at $1 \mu\text{M}$ concentration, and recapitulate the behaviour of the ΔsapM strain in macrophage infections²⁴ (and this study). These results are consistent with the critical role of SapM in phagosomal maturation arrest to increase Mtb survival and pathogenesis, and with the reported reduction of mycobacterial burden both in vitro^{12,13} and in vivo^{17,18}, when inhibiting MptpB, another secreted virulence factor. Notably, we see also reduction in intracellular burden of *F. tularensis* when using compound **1**, suggesting the potential of developing antivirulence agents with a broad-spectrum activity to treat different microbial infections. This is the first report of potent inhibitors of SapM and provides a basis for further development to exploit the potential of this target in the treatment of TB.

Materials and methods

Production of recombinant proteins. SapM was expressed in *Escherichia coli* C41 (DE3) by auto-induction at 20°C for 24 h as previously described^{22,53}. The C-terminal his-tagged SapM was purified by nickel affinity chromatography and eluted with 50 mM HEPES, 500 mM NaCl, 0.05% sarkosyl, 200 mM imidazole and 3 mM ethylenediaminetetraacetic acid (EDTA), pH 7. MptpA and MptpB were expressed in *E. coli* BL21(DE3) at 18°C with 0.5 mM isopropyl- β -D-thiogalactopyranoside (IPTG) for MptpB and 0.1 mM IPTG for MptpA for 16 h¹⁸. MptpA and MptpB were both purified by nickel affinity chromatography followed by size exclusion in a Superdex75 (10/300) column (GE Healthcare) eluted with 20 mM Tris-Base, 150 mM NaCl and 3 mM EDTA, pH 7¹⁸. The full-length hPTP1B and hVHR proteins were expressed in *E. coli* BL21(DE3) at 18°C with 0.5 mM IPTG for 16 h¹⁸. hPTP1B and hVHR were both purified using Glutathione Sepharose 4B beads (GE Healthcare) eluted with 20 mM HEPES, 500 mM NaCl, 5 mM dithiothreitol (DTT) and 10 mM glutathione (GSH), pH 7.

Compound screening. Four libraries were selected for screening: (1) in-house compounds (96), (2) LOPAC-Pfizer library (90), (3) Enzo-BML-2834 library (32) and (4) LOPAC-1280 library (1273). LOPAC-Pfizer and LOPAC-1280 libraries were purchased from Sigma-Aldrich and the Enzo-BML-2834 library from Enzo Life Sciences. In addition, seven Tyrphostin analogues and five polyphenols were purchased from Enzo Life Sciences, Cambridge Bioscience or Sigma-Aldrich. Inhibition of SapM was tested using the *p*-nitrophenyl phosphate (*p*NPP) assay. A 150 μl of reaction mixture contained 0.5 μg of SapM protein in 50 mM Tris-Base, 150 mM NaCl, pH 7.5 and 100 μM of compounds, followed by the addition of *p*NPP (at its K_m concentration). The reaction mixture was incubated for 30 min at 37°C and quenched with 50 μl of 1 M NaOH. Production of *p*-nitrophenol (*p*NP) was measured at 405 nm using a Multiskan Spectrum spectrophotometer (Thermo Scientific) and quantified using a *p*NP standard curve (15–2000 μM of *p*NP). Specific activity (SA) was calculated as nmol of *p*NP generated per μg of protein over the reaction time. Activity towards MptpA, MptpB, hPTP1B, and hVHR with the *p*NPP assay was performed in 50 mM Tris-Base, 50 mM Bis-Tris, 100 mM Sodium Acetate (pH 6 for MptpA and MptpB, and pH 5.5 for hPTP1B and hVHR) and incubated at 37°C for 15 min¹⁸. The Michaelis–Menten parameters K_m and V_{max} were calculated using non-linear regression fit in GraphPad Prism 8.41. IC_{50} values were determined using inhibitor concentrations 0–500 μM and values calculated using a four-parameter non-linear regression fit in GraphPad Prism 8.41.

To determine the type of inhibition different inhibitor concentrations were selected to yield around 30% and 75% inhibition for each concentration of *p*NPP. This ensures sufficient signal to obtain accurate data while allowing a significant inhibition effect⁴⁸. Velocity (*V*) was plotted as a function of *p*NPP concentration and fit in a Lineweaver–Burk plot (double-reciprocal) using GraphPad Prism 8.41. All assays were done in 96-well microplates and performed in triplicate in at least two independent experiments.

Bacterial and cell culture. THP-1 monocyte cell lines (ATCC) were cultured in Roswell Park Memorial Institute-1640 medium (RPMI) (R8758-Sigma-Aldrich) containing L-glutamine supplemented with 10% heat inactivated fetal bovine serum (FBS, Invitrogen) at 37°C in 5% CO_2 . Mtb strain H37Rv was grown in Middlebrook 7H9 broth (BD Diagnostics) or on Middlebrook 7H10 agar, both supplemented with 0.05% Tween 80, 0.2% glycerol and 10% OADC (Oleic Albumin Dextrose Catalase from Becton Dickinson Microbiology Systems) at 37°C in 5% CO_2 . Mtb cultures were prepared using 1 ml of mid-log phase Mtb stock into 20 ml of fresh media and incubated static for 6 days prior to being used in infection or acellular assays.

Cytotoxicity assays. A colorimetric assay using the tetrazolium dye 3-(4,5-dimethylthiazol-2-yl)-2,5-diphenyltetrazolium bromide (MTT) was performed as described previously⁵⁴. THP-1 monocytes cell lines were seeded in 96-well cell culture plates, flat bottom (Corning) at a density of 5×10^4 (in 200 μl media) and treated with 200 nM of phorbol 12-myristate-13-acetate (PMA) for 2 h, then media was replaced with fresh RPMI (containing 10% FBS) and cells incubated overnight. The following day media was replaced with fresh RPMI (containing 10% FBS) with 10 and 40 μM of compound **1**, **2** or **13**. This was repeated at 24 h, and at 48 h cells were washed with Dulbecco's phosphate buffered saline (PBS) and fresh RPMI without inhibitors added. For the MH-S cells (ATCC, CRL-2019), an SV40-transformed alveolar macrophage cell line, 6×10^3 cells (in 200 μl media) were seeded in 96-well cell culture plates and incubated overnight. Treatment was performed only for 24 h. Cell viability was assessed at 24 h (MH-S) or 72 h (THP-1) by adding MTT (5 mg/ml in PBS) and incubated 2 h at 37°C in 5% CO_2 . Media was removed followed by addition of 200 μl of dimethyl sulfoxide (DMSO) and 25 μl of Sorensen's glycine buffer, and absorbance measured at 570 nm. Each assay was performed in trip-

licate in at least three independent experiments. A compound was considered toxic when macrophage viability was < 70%.

***Mycobacterium tuberculosis* infection assay.** THP-1 monocytes were seeded in 24-well cell culture plates, flat bottom (Corning) at a density of 1×10^5 cells per well (in 500 μ l media) and treated with 200 nM PMA for 2 h, then media was replaced with fresh RPMI (with 10% FBS) and cells incubated overnight. The following day, media was replaced with fresh RPMI containing compounds at 1 and 40 μ M dissolved in DMSO. Cells were infected with a multiplicity of infection (MOI) of 5:1 (bacteria:macrophage). After 4 h of infection, THP-1 cells were washed three times with PBS and fresh RPMI was added containing the inhibitors, and this was repeated at 24 h. At 24 h or 72 h, cells were lysed with 400 μ l of ice-cold distilled water and together with the cell-pelleted supernatants were plated onto 7H10 agar. All experimental points were plated as tenfold dilutions in triplicate in at least two independent experiments. Colonies were counted after 14 days. Data is plotted as fold change of Mtb burden calculated from the average CFU/ml at 24 h or 72 h. A negative control of DMSO was included. Statistical significance was evaluated by one-way ANOVA followed by a multiple comparison analyses of variance by Dunnett's test (GraphPad Prism 8.41 for Windows). Differences were considered significant at the 95% level of confidence. All experiments with Mtb were carried out in a biosafety level 3 containment facility. Note that resting macrophages were used in the Mtb infections to mimic a susceptible host (where activation may be impaired).

***Francisella tularensis* infection assay.** *Francisella tularensis* live vaccine strain (LVS), belonging to subspecies *holarctica* was used as described³⁵. Briefly, to achieve the inoculum *F. tularensis* from a blood cysteine glucose agar (BCGA) plate grown for 48 h at 37 °C was resuspended in complete L-15 media (10% FCS, 5 mM L-Glutamine) (Life Technologies) to a 600 nm spectrophotometer optical density (OD) reading of 0.20 which corresponded to $\sim 1 \times 10^9$ CFU/ml. MOI of 100 was achieved through serial dilutions and inoculum determined by plate count on BCGA.

MH-S cells (ATCC, CRL-2019), an SV40-transformed alveolar macrophage cell line, were incubated for 2 h with the *F. tularensis* MOI 100 (bacteria:macrophage) at 37 °C to allow for cellular uptake of the bacteria. This was in the presence or absence of compound **1** (1 and 40 μ M) and DMSO control. *F. tularensis* was removed and cells were washed with warm PBS, followed by 30 min incubation with 10 μ g/ml gentamicin (Sigma-Aldrich) to kill any extracellular bacteria and then replaced with complete L-15 with 2 μ g/ml gentamicin and compound **1** (1 or 40 μ M) or DMSO control for 24 h. At 24 h cells were lysed with 4 °C water to determine bacterial burden. Statistical significance was evaluated by one-way ANOVA followed by a multiple comparison analyses of variance by Dunnett's test (GraphPad Prism 8.41 for Windows). Differences were considered significant at the 95% level of confidence. All experiments with *F. tularensis* were carried out in a biosafety level 3 containment facility.

Acellular growth of *Mycobacterium tuberculosis* and *Francisella tularensis*. Mtb (4.4×10^7 CFUs) was cultured in 25 ml of Middlebrook 7H9 and compounds **1**, **2** or **13** at 40 μ M were added on day 0. Cultures were grown static over 9 days at 37 °C in 5% CO₂. Controls were DMSO only and isoniazid at 0.14 μ g/ml. *F. tularensis* (1×10^8 CFUs) was cultured in complete L-15 media (10% FCS) at 37 °C for 24 h in the presence or absence of compound **1** at 40 μ M. Bacterial growth was monitored by OD at 600 nm. Experiments were performed in triplicate on at least two separate studies. Statistical significance was evaluated by two-way ANOVA followed by multiple comparison analyses of variance by Bonferroni test (GraphPad Prism 8.41 for Windows). Differences were considered significant at the 95% level of confidence.

Received: 16 July 2020; Accepted: 15 February 2021

Published online: 07 April 2021

References

1. World Health Organization. *Global Tuberculosis Report* (2019). <https://apps.who.int/iris/bitstream/handle/10665/329368/9789241565714-eng.pdf?ua=1>. Accessed 15 June 2020.
2. Diacon, A. H. *et al.* Multidrug-resistant tuberculosis and culture conversion with bedaquiline. *N. Engl. J. Med.* **371**, 723–732. <https://doi.org/10.1056/NEJMoa1313865> (2014).
3. Gler, M. T. *et al.* Delamanid for multidrug-resistant pulmonary tuberculosis. *N. Engl. J. Med.* **366**, 2151–2160. <https://doi.org/10.1056/NEJMoa1112433> (2012).
4. Bloemberg, G. V. *et al.* Acquired resistance to bedaquiline and delamanid in therapy for tuberculosis. *N. Engl. J. Med.* **373**, 1986–1988. <https://doi.org/10.1056/NEJMc1505196> (2015).
5. Somoskovi, A., Bruderer, V., Hönke, R., Bloemberg, G. V. & Böttger, E. C. A mutation associated with clofazimine and bedaquiline cross-resistance in MDR-TB following bedaquiline treatment. *Eur. Respir. J.* **45**, 554–557. <https://doi.org/10.1183/09031936.00142914> (2015).
6. Fujiwara, M., Kawasaki, M., Hariguchi, N., Liu, Y. & Matsumoto, M. Mechanisms of resistance to delamanid, a drug for *Mycobacterium tuberculosis*. *Tuberculosis* **108**, 186–194. <https://doi.org/10.1016/j.tube.2017.12.006> (2018).
7. Nguyen, T. V. A. *et al.* Bedaquiline resistance: Its emergence, mechanism, and prevention. *Clin. Infect. Dis.* **66**, 1625–1630. <https://doi.org/10.1093/cid/cix992> (2018).
8. Clatworthy, A. E., Pierson, E. & Hung, D. T. Targeting virulence: A new paradigm for antimicrobial therapy. *Nat. Chem. Biol.* **3**, 541–548. <https://doi.org/10.1038/nchembio.2007.24> (2007).
9. Rasko, D. A. & Sperandio, V. Anti-virulence strategies to combat bacteria-mediated disease. *Nat. Rev. Drug Discov.* **9**, 117–128. <https://doi.org/10.1038/nrd3013> (2010).
10. Dickey, S. W., Cheung, G. Y. C. & Otto, M. Different drugs for bad bugs: Antivirulence strategies in the age of antibiotic resistance. *Nat. Rev. Drug Discov.* **16**, 457–471. <https://doi.org/10.1038/nrd.2017.23> (2017).

11. Theuretzbacher, U. & Piddock, L. J. V. Non-traditional antibacterial therapeutic options and challenges. *Cell Host Microbe* **26**, 61–72. <https://doi.org/10.1016/j.chom.2019.06.004> (2019).
12. Beresford, N. J. *et al.* Inhibition of MptpB phosphatase from *Mycobacterium tuberculosis* impairs mycobacterial survival in macrophages. *J. Antimicrob. Chemother.* **63**, 928–936. <https://doi.org/10.1093/jac/dkp031> (2009).
13. Zhou, B. *et al.* Targeting mycobacterium protein tyrosine phosphatase B for antituberculosis agents. *Proc. Natl. Acad. Sci.* **107**, 4573–4578. <https://doi.org/10.1073/pnas.0909133107> (2010).
14. Paolino, M. *et al.* Development of potent inhibitors of the *Mycobacterium tuberculosis* virulence factor Zmp1 and evaluation of their effect on mycobacterial survival inside macrophages. *ChemMedChem* **13**, 422–430. <https://doi.org/10.1002/cmdc.201700759> (2018).
15. Johnson, B. K. & Abramovitch, R. B. Small molecules that sabotage bacterial virulence. *Trends Pharmacol. Sci.* **38**, 339–362. <https://doi.org/10.1016/j.tips.2017.01.004> (2017).
16. Kanehiro, Y. *et al.* Identification of novel mycobacterial inhibitors against mycobacterial protein kinase G. *Front. Microbiol.* **9**, 31. <https://doi.org/10.3389/fmicb.2018.01517> (2018).
17. Dutta, N. K. *et al.* Mycobacterial protein tyrosine phosphatases A and B inhibitors augment the bactericidal activity of the standard anti-tuberculosis regimen. *ACS Infect. Dis.* **2**, 231–239. <https://doi.org/10.1021/acinfed.5b00133> (2016).
18. Vickers, C. F. *et al.* Structure-based design of MptpB inhibitors that reduce multidrug-resistant *Mycobacterium tuberculosis* survival and infection burden in vivo. *J. Med. Chem.* **61**, 8337–8352. <https://doi.org/10.1021/acs.jmedchem.8b00832> (2018).
19. Cole, S. T. Inhibiting *Mycobacterium tuberculosis* within and without. *Philos. Trans. R. Soc. Biol. Sci.* **371**, 20150506. <https://doi.org/10.1098/rstb.2015.0506> (2016).
20. Libardo, M. D. J., Boshoff, H. I. & Barry, C. E. The present state of the tuberculosis drug development pipeline. *Curr. Opin. Pharmacol.* **42**, 81–94. <https://doi.org/10.1016/j.coph.2018.08.001> (2018).
21. Theuretzbacher, U. *et al.* Analysis of the clinical antibacterial and antituberculosis pipeline. *Lancet Infect. Dis.* **19**, e40–e50. [https://doi.org/10.1016/S1473-3099\(18\)30513-9](https://doi.org/10.1016/S1473-3099(18)30513-9) (2019).
22. Fernandez-Soto, P., Bruce, A. J. E., Fielding, A. J., Cavet, J. S. & Taberner, L. Mechanism of catalysis and inhibition of *Mycobacterium tuberculosis* SapM, implications for the development of novel antivirulence drugs. *Sci. Rep.* **9**, 10315. <https://doi.org/10.1038/s41598-019-46731-6> (2019).
23. Saikolappan, S. *et al.* The fbpA/sapM double knock out strain of *Mycobacterium tuberculosis* is highly attenuated and immunogenic in macrophages. *PLoS ONE* **7**, e36198. <https://doi.org/10.1371/journal.pone.0036198> (2012).
24. Puri, R. V., Reddy, P. V. & Tyagi, A. K. Secreted acid phosphatase (SapM) of *Mycobacterium tuberculosis* is indispensable for arresting phagosomal maturation and growth of the pathogen in guinea pig Tissues. *PLoS ONE* **8**, e70514. <https://doi.org/10.1371/journal.pone.0070514> (2013).
25. Saleh, M. T. & Belisle, J. T. Secretion of an acid phosphatase (SapM) by *Mycobacterium tuberculosis* that is similar to eukaryotic acid phosphatases. *J. Bacteriol.* **182**, 6850–6853. <https://doi.org/10.1128/JB.182.23.6850-6853.2000> (2000).
26. Ellis, J., Oyston, P. C. F., Green, M. & Titball, R. W. Tularemia. *Clin. Microbiol. Rev.* **15**, 631–646. <https://doi.org/10.1128/CMR.15.4.631> (2002).
27. Reilly, T. J., Baron, G. S., Nano, F. E. & Kuhlenschmidt, M. S. Characterization and sequencing of a respiratory burst-inhibiting acid phosphatase from *Francisella tularensis*. *J. Biol. Chem.* **271**, 10973–10983. <https://doi.org/10.1074/jbc.271.18.10973> (1996).
28. Reilly, T. J., Felts, R. L., Henzl, M. T., Calcutt, M. J. & Tanner, J. J. Characterization of recombinant *Francisella tularensis* acid phosphatase A. *Protein Expr. Purif.* **45**, 132–141. <https://doi.org/10.1016/j.pep.2005.05.001> (2006).
29. Mohapatra, N. P., Balagopal, A., Soni, S., Schlesinger, L. S. & Gunn, J. S. AcpA is a *Francisella* acid phosphatase that affects intramacrophage survival and virulence. *Infect. Immunol.* **75**, 390–396. <https://doi.org/10.1128/IAI.01226-06> (2007).
30. Waybright, T. J., Britt, J. R. & McCloud, T. G. Overcoming problems of compound storage in DMSO: Solvent and process alternatives. *J. Biomol. Screen.* **14**, 708–715. <https://doi.org/10.1177/1087057109335670> (2009).
31. Pott, A. *et al.* Therapeutic chemical screen identifies phosphatase inhibitors to reconstitute PKB phosphorylation and cardiac contractility in ILK-deficient zebrafish. *Biomolecules* **8**, 153. <https://doi.org/10.3390/biom8040153> (2018).
32. Evers, B. *et al.* A high throughput pharmaceutical screen identifies compounds with specific toxicity against BRCA2-deficient tumors. *Nat. Rev. Cancer* **16**, 99–108. <https://doi.org/10.1158/1078-0432.CCR-09-2434.A> (2010).
33. Laskowski, R. A., Gerick, F. & Thornton, J. M. The structural basis of allosteric regulation in proteins. *FEBS Lett.* **583**, 1692–1698. <https://doi.org/10.1016/j.febslet.2009.03.019> (2009).
34. Gazit, A., Yaish, P., Gilon, C. & Levitzki, A. Tyrosinase I: Synthesis and biological activity of protein tyrosine kinase inhibitors. *J. Med. Chem.* **32**, 2344–2352. <https://doi.org/10.1021/jm00130a020> (1989).
35. Kim, D. J. *et al.* Novel TOPK inhibitor HI-TOPK-032 effectively suppresses colon cancer growth. *Cancer Res.* **72**, 3060–3068. <https://doi.org/10.1158/0008-5472.CAN-11-3851> (2012).
36. Marchesi, S. *et al.* DEPDC1B coordinates de-adhesion events and cell-cycle progression at mitosis. *Dev. Cell* **31**, 420–433. <https://doi.org/10.1016/j.devcel.2014.09.009> (2014).
37. Manerba, M. *et al.* Galloflavin (CAS 568–80–9): A novel inhibitor of lactate dehydrogenase. *ChemMedChem* **7**, 311–317. <https://doi.org/10.1002/cmdc.201100471> (2012).
38. Miyake, A. *et al.* Suppression of inflammatory responses to 12-O-tetradecanoylphorbol-13-acetate and carrageenin by YM-26734, a selective inhibitor of extracellular group II phospholipase A2. *Br. J. Pharmacol.* **110**, 447–453. <https://doi.org/10.1111/j.1476-5381.1993.tb13831.x> (1993).
39. Hoshiga, M. & Hatakeyama, K. Enzymatic synthesis of 6R-[U-14C]tetrahydrobiopterin from [U-14C]GTP. *Methods Enzymol.* **281**, 123–129. [https://doi.org/10.1016/S0076-6879\(97\)81017-8](https://doi.org/10.1016/S0076-6879(97)81017-8) (1997).
40. Robbins, I. M. *et al.* Safety of sapropterin dihydrochloride (6R-BH4) in patients with pulmonary hypertension. *Exp. Lung Res.* **37**, 26–34. <https://doi.org/10.3109/01902148.2010.512972> (2011).
41. Stadlbauer, S., Rios, P., Ohmori, K., Suzuki, K. & Köhn, M. Procyanidins negatively affect the activity of the phosphatases of regenerating liver. *PLoS ONE* **10**, 1–18. <https://doi.org/10.1371/journal.pone.0134336> (2015).
42. Lipinski, C. A., Lombardo, F., Dominy, B. W. & Feeney, P. J. Experimental and computational approaches to estimate solubility and permeability in drug discovery and development settings. *Adv. Drug Deliv. Rev.* **46**, 3–26. <https://doi.org/10.1016/j.addr.2012.09.019> (2011).
43. Umezawa, H. *et al.* Studies on a new epidermal growth factor-receptor kinase inhibitor, erbstatin, produced by MH435-hF3. *J. Antibiot. (Tokyo)* **39**, 170–173. <https://doi.org/10.7164/antibiotics.39.170> (1986).
44. Beresford, N. *et al.* MptpB, a virulence factor from *Mycobacterium tuberculosis*, exhibits triple-specificity phosphatase activity. *Biochem. J.* **406**, 13–18. <https://doi.org/10.1042/BJ20070670> (2007).
45. Koul, A. *et al.* Cloning and characterization of secretory tyrosine phosphatases of *Mycobacterium tuberculosis*. *J. Bacteriol.* **182**, 5425–5432. <https://doi.org/10.1128/JB.182.19.5425-5432.2000> (2000).
46. Cowley, S. C., Babakaiff, R. & Av-Gay, Y. Expression and localization of the *Mycobacterium tuberculosis* protein tyrosine phosphatase PtpA. *Res. Microbiol.* **153**, 233–241. [https://doi.org/10.1016/S0923-2508\(02\)01309-8](https://doi.org/10.1016/S0923-2508(02)01309-8) (2002).
47. Wong, D., Bach, H., Sun, J., Hmama, Z. & Av-Gay, Y. *Mycobacterium tuberculosis* protein tyrosine phosphatase (PtpA) excludes host vacuolar-H⁺-ATPase to inhibit phagosome acidification. *Proc. Natl. Acad. Sci. U.S.A.* **108**, 19371–19376. <https://doi.org/10.1073/pnas.1109201108> (2011).

48. Copeland, R. A. Reversible inhibitors. In *Enzymes: A Practical Introduction to Structure, Mechanism, and Data Analysis* (ed. Copeland, R. A.) 266–303 (Wiley-VCH, 2000).
49. Ni, M., Pan, J., Hu, X., Gong, D. & Zhang, G. Inhibitory effect of corosolic acid on α -glucosidase: Kinetics, interaction mechanism, and molecular simulation. *J. Sci. Food Agric.* **378**, 9862. <https://doi.org/10.1002/jsfa.9862> (2019).
50. Heise, C. E. *et al.* Mechanistic and structural understanding of uncompetitive inhibitors of caspase-6. *PLoS ONE* **7**, e50864. <https://doi.org/10.1371/journal.pone.0050864> (2012).
51. Vrbanac, J. & Slauter, R. ADME in drug discovery. In *A Comprehensive Guide to Toxicology in Preclinical Drug Development* (eds Vrbanac, J. & Slauter, R.) 3–30 (Elsevier, 2013).
52. Mcrae, S. *et al.* Inhibition of AcpA phosphatase activity with ascorbate attenuates *Francisella tularensis* intramacrophage survival. *J. Biol. Chem.* **285**, 5171–5177. <https://doi.org/10.1074/jbc.M109.039511> (2010).
53. Fernandez-Soto, P., Cavet, J. S. & Tabernero, L. Expression and purification of soluble recombinant SapM from *Mycobacterium tuberculosis*. *Protein Expr. Purif.* <https://doi.org/10.1016/j.pep.2020.105663> (2020).
54. Mosmann, T. Rapid colorimetric assay for cellular growth and survival: Application to proliferation and cytotoxicity assays. *J. Immunol. Methods* **65**, 55–63. [https://doi.org/10.1016/0022-1759\(83\)90303-4](https://doi.org/10.1016/0022-1759(83)90303-4) (1983).
55. Casulli, J. *et al.* CD200R deletion promotes a neutrophil niche for *Francisella tularensis* and increases infectious burden and mortality. *Nat. Commun.* **10**, 1–9. <https://doi.org/10.1038/s41467-019-10156-6> (2019).

Acknowledgements

This study was supported by funding from SENESCYT-Ecuador with a studentship award to P.F.S and D.S.C, by a Medical Research Council, UK confidence in concept award to LT (MC_PC_18056) and a BBSRC grant to LT and JSC (BB/T00083X/1). We thank Benjamin Thornton for advice on scaffold and SAR analysis, Karen Garcia for support with the macrophage infections, and the biomolecular analysis core facility of the University of Manchester.

Author contributions

P.F.-S. designed the experiments, produced the data, analysed and discussed the results and wrote the manuscript; J.C. produced the data of *F. tularensis* infection experiments; D.S.-C. performed screening of polyphenols from published literature; P.R.-F. performed delta sapM infections and analysed data; T.J. performed MST experiments and analysed data; M.A.T. and J.S.C. supervised part of the work and edited the manuscript; L.T. directed the study, analysed and discussed the data and edit the manuscript. All authors have read and approved the final manuscript.

Competing interests

The authors declare no competing interests.

Additional information

Supplementary Information The online version contains supplementary material available at <https://doi.org/10.1038/s41598-021-87117-x>.

Correspondence and requests for materials should be addressed to L.T.

Reprints and permissions information is available at www.nature.com/reprints.

Publisher's note Springer Nature remains neutral with regard to jurisdictional claims in published maps and institutional affiliations.



Open Access This article is licensed under a Creative Commons Attribution 4.0 International License, which permits use, sharing, adaptation, distribution and reproduction in any medium or format, as long as you give appropriate credit to the original author(s) and the source, provide a link to the Creative Commons licence, and indicate if changes were made. The images or other third party material in this article are included in the article's Creative Commons licence, unless indicated otherwise in a credit line to the material. If material is not included in the article's Creative Commons licence and your intended use is not permitted by statutory regulation or exceeds the permitted use, you will need to obtain permission directly from the copyright holder. To view a copy of this licence, visit <http://creativecommons.org/licenses/by/4.0/>.

© The Author(s) 2021